Afdelingen for Bærende Konstruktioner
Department of Structural Engineering
Danmarks Tekniske Universitet • Technical University of Denmark

The HOTCH-POTCH Disk Element - Finite Element for Analysis of Reinforced Concrete Disks

Lars Jagd

Jens Christoffersen

M.P. Nielsen

Serie R No 317 1994

The HOTCH-POTCH Disk Element - Finite Element for Analysis of Reinforced Concrete Disks

Lars Jagd

Jens Christoffersen

M.P. Nielsen

The HOTCH-POTCH Disk Element - Finite Element for Analysis of Reinforced Concrete Disks

Tryk:
Afdelingen for Bærende Konstruktioner
Danmarks Tekniske Universitet
Lyngby
ISBN 87-7740-153-0
ISSN 0909-587X
Bogbinder:
H. Meyer, Bygning 101, DTU

Abstract

The report describes a new disk element, used for finite element analysis, which is based on a simple, mechanical model, that causes normal stresses to be concentrated in stringers along the element edges and shear to be transferred by a constant in-plane shear stress field.

The element has a transparent behavior very similar to the stringer method, and the constant shear stress within each element makes it well-suited for analyses and design of reinforced concrete disks.

The element has been implemented in a finite element programme. Input and output is of a form that can easily be converted to typical reinforcement detailing.

A number of test problems have been analyzed and the results compared with various theoretical results as well as with another FEM programme. All the problems yield very accurate results, the computational efforts taken into account.

Table of Contents

Chapter 1

Introduction

In this report elastic disks are examined. In general, disks are plane structures which carry external loads by in-plane actions. In the literature analytical solutions can only be found for quite simple geometries. Therefore disks are most often designed using simplified hand calculation methods or various numerical methods.

A commonly used hand calculation method for analyzing concrete disks in the serviceability as well as the ultimate limit states is the stringer method. However, this method cannot be used for calculating deformations and crack widths. Typically reinforcement in the serviceability state is applied based on code practice and common engineering judgement.

Among the numerical methods, the finite element methods are by far the most prevalent today. This is due to the fact, that the finite element method is very suitable for implementation in computer programmes. Furthermore, the commercial FEM programmes are often coupled to advanced pre- and postprocessors making them very user-friendly.

The significance of FEM programmes for analyses of complex structures is undisputed. However, it is important to consider the basic assumptions of the programme and the elements used, before the numerical results obtained may be accepted as reasonable approximations to the actual conditions.

In this report a new disk finite element is described. The element is based on a simple, mechanical model, that causes normal stresses to be concentrated in stringers along the element edges and shear to be transferred by a constant in-plane shear stress field. The element has a transparent behavior very analogue to the stringer method, and the constant shear stress within each element makes it well-suited for analyses and design of reinforced concrete disks.

Chapter 2

The HP Disk Element

2.1 General

The HP disk element is based on a simple, mechanical model that causes normal stresses to be concentrated in stringers along the element edges and shear to be transferred by a constant in-plane shear stress field. In this section the stiffness matrix for such an element will be derived. The element is defined from four corner nodes as seen on figure 2.1. The points *A-D* also seen on the figure, define the midpoints of the four edges. The edge lengths are given by l_1 and l_2 and the reinforcement ratios by ρ_1-ρ_4.

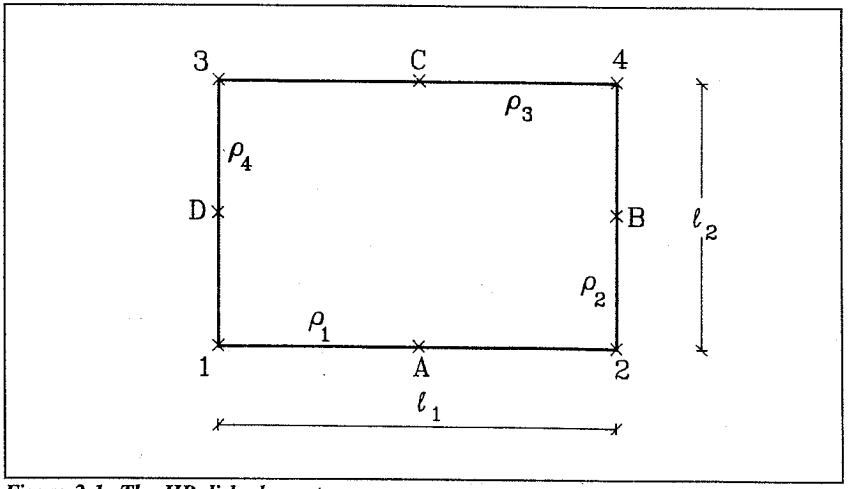

Figure 2.1: The HP disk element.

In each of the four corner nodes two translational degrees of freedom are introduced. Thus an element has eight degrees of freedom named u_1-u_8, see figure 2.2.

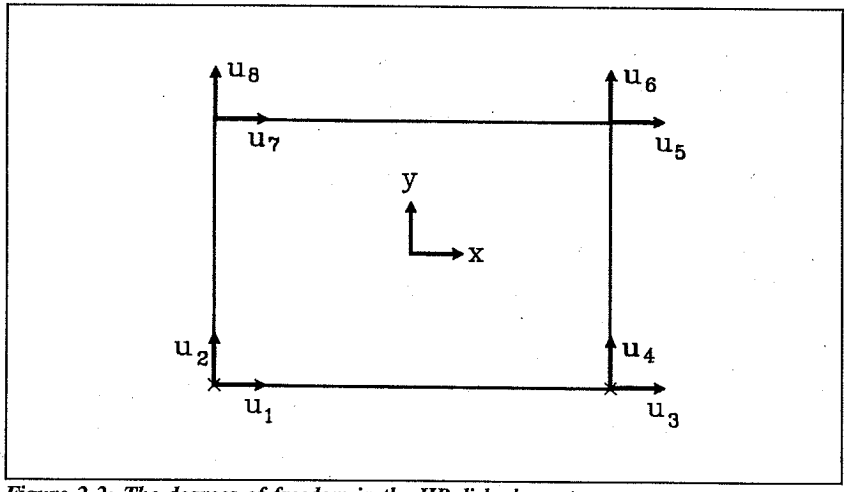

Figure 2.2: The degrees of freedom in the HP disk element.

The displacements at the midpoint of each of the four edges are referred to as U_1-U_8 and are calculated from u_1-u_8 as given in equation **(2.1)**.

$$\begin{aligned} U_1 &= \frac{1}{2}\cdot(u_1 + u_3), \quad U_2 = \frac{1}{2}\cdot(u_2 + u_4) \\ U_3 &= \frac{1}{2}\cdot(u_3 + u_5), \quad U_4 = \frac{1}{2}\cdot(u_4 + u_6) \\ U_5 &= \frac{1}{2}\cdot(u_5 + u_7), \quad U_6 = \frac{1}{2}\cdot(u_6 + u_8) \\ U_7 &= \frac{1}{2}\cdot(u_1 + u_7), \quad U_8 = \frac{1}{2}\cdot(u_2 + u_8) \end{aligned} \tag{2.1}$$

2.2 The Element Stiffness Matrix

An infinitesimal element limited by four sections with normals in the x- and y-directions is considered, se figure 2.3. The disk stresses are the two normal stresses σ_x and σ_y and the shear stress τ_{xy}.

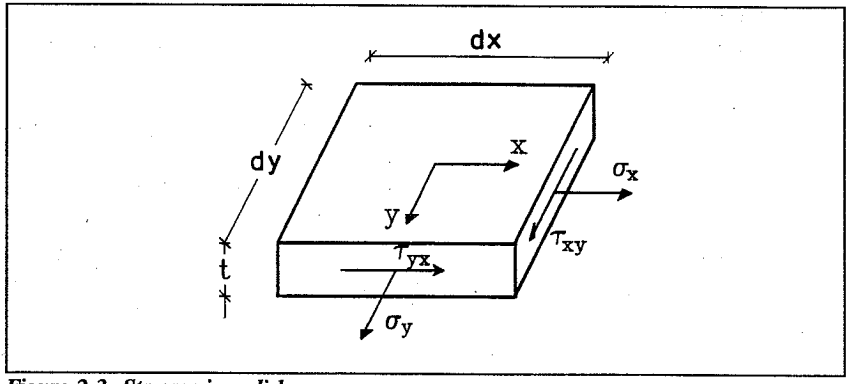

Figure 2.3: Stresses in a disk.

In order to determine the terms in the element stiffness matrix $\underline{k}$, the normal- and shear stiffnesses are considered. The normal stiffnesses are concentrated in stringers along the four edges of the element. The normal stiffness of a stringer depends on whether the normal stress is tensile or compressive. If the normal force in the stringer between node 1 and 2, S_{12}, is tensile the normal stiffness in this stringer is determined from the reinforcement ratio ρ_1, Young's Modulus of the steel E_s and the element edge lengths as given in **(2.2)**.

$$k_1 = E_s \cdot \rho_1 \cdot \frac{l_2}{2} \cdot \frac{1}{l_1} \qquad \textbf{(2.2)}$$

If the normal force S_{12} is compressive, the normal stiffness is determined from the disk thickness t, Young's Modulus of the concrete E_c and the element edge lengths as given in **(2.3)**.

$$k_1 = E_c \cdot t \cdot \frac{l_2}{2} \cdot \frac{1}{l_1} \tag{2.3}$$

Likewise the normal stiffnesses k_2-k_4 of the other stringers S_{23}, S_{34} and S_{41} are determined. It should be noted, that the stiffnesses are determined independently. Thus it is possible for e.g. stringer S_{23} to be in tension while stringer S_{41} is in compression.

Generally, the change of angle ϕ_{xy} is given from the following expression:

$$\phi_{xy} = \frac{\partial u_x}{\partial y} + \frac{\partial u_y}{\partial x} \tag{2.4}$$

As the shear stress and thus the change of angle within one element is assumed to be constant, the two terms in **(2.4)** are determined from the mean displacements U_1-U_8:

$$\begin{aligned} \frac{\partial u_x}{\partial y} &= \frac{U_5 - U_1}{l_2} \\ \frac{\partial u_y}{\partial x} &= \frac{U_4 - U_8}{l_1} \end{aligned} \tag{2.5}$$

Combining **(2.1)**, **(2.4)** and **(2.5)**, the change of angle can be determined from the nodal displacements u_1-u_8 by:

$$\phi_{xy} = \frac{u_5 + u_7 - u_1 - u_3}{2 \cdot l_2} + \frac{u_4 + u_6 - u_2 - u_8}{2 \cdot l_1} \tag{2.6}$$

In the following section, the contributions to the element stiffness matrix from the shear stiffnesses will be determined. The term k_{ij} is determined as the load corresponding to the degree of freedom i, that must be applied in node i in order to obtain a deformation of *1* in the direction of the degree of freedom j.

First, the contributions to k_{ij} are determined. The following virtual displacement condition is chosen:

$$u_1 = 1$$
$$u_i = 0, \quad i = [2,3,....,8] \tag{2.7}$$

The contribution from the constant in-plane shear stress is concentrated in the nodes as the forces P_1-P_8, see figure 2.4.

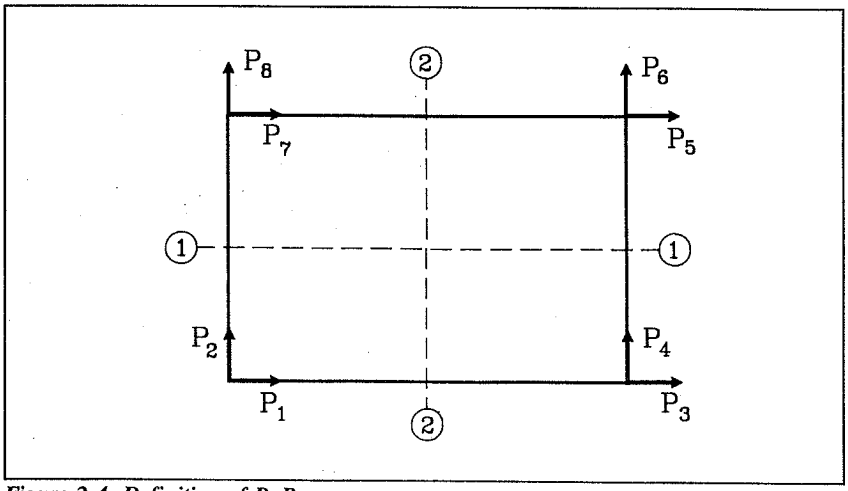

Figure 2.4: Definition of P_1-P_8.

Combining **(2.6)** and **(2.7)**, the change of angle ϕ_{xy} is given by **(2.8)**:

$$\phi_{xy} = -\frac{1}{2 \cdot l_2} \tag{2.8}$$

The external work A_e is determined by the force P_1 and the displacement u_1:

$$A_e = P_1 \cdot 1 \tag{2.9}$$

while the internal work A_i is a function of the disk thickness t, the shear stress τ_{xy} and the change of angle ϕ_{xy}:

$$A_i = t \cdot \int_{el} \tau_{xy} \cdot \phi_{xy} \, dx\,dy \tag{2.10}$$

However, τ_{xy} can also be expressed as:

$$\tau_{xy} = \phi_{xy} \cdot G \tag{2.11}$$

where G is the shear modulus which is assumed constant in each element. Combining **(2.10)** and **(2.11)** the internal work A_i can be expressed as:

$$\begin{aligned} A_i &= t \cdot \int_{el} \tau_{xy} \cdot \phi_{xy} \, dx\,dy \\ &= t \cdot \int_{el} \phi_{xy} \cdot G \cdot \phi_{xy} \, dx\,dy \\ &= t \cdot G \cdot \int_{el} \phi_{xy}^2 \, dx\,dy \end{aligned} \tag{2.12}$$

By combining **(2.8)**, **(2.9)** and **(2.12)**, P_1 can be determined by putting the internal work equal to the external work:

$$P_1 = \frac{1}{4} \cdot G \cdot t \cdot \frac{l_1}{l_2} \tag{2.13}$$

In order to determine P_3, P_5 and P_7, the equations **(2.14)-(2.16)** are used. The sum of the forces equals zero:

$$P_1 + P_3 + P_5 + P_7 = 0 \qquad \textbf{(2.14)}$$

Equilibrium in section 1-1 (in the x-direction), see figure 2.4:

$$P_7 + P_5 = \tau_{xy} \cdot l_1 \cdot t = -\frac{1}{2} \cdot G \cdot t \cdot \frac{l_1}{l_2} \qquad \textbf{(2.15)}$$

Equilibrium in section 2-2 (in the x-direction):

$$P_3 + P_5 = 0 \qquad \textbf{(2.16)}$$

By solving these three equations with three unknowns, **(2.17)** is obtained:

$$\begin{aligned} P_3 &= \frac{1}{4} \cdot G \cdot t \cdot \frac{l_1}{l_2} \\ P_5 &= -\frac{1}{4} \cdot G \cdot t \cdot \frac{l_1}{l_2} \\ P_7 &= -\frac{1}{4} \cdot G \cdot t \cdot \frac{l_1}{l_2} \end{aligned} \qquad \textbf{(2.17)}$$

In order to determine P_2, P_4, P_6 and P_8, only three equations **(2.18)-(2.20)** are available. The sum of the forces is zero:

$$P_2 + P_4 + P_6 + P_8 = 0 \qquad \textbf{(2.18)}$$

Equilibrium in section 1-1 (in the y-direction):

$$P_2 + P_4 = 0 \tag{2.19}$$

Equilibrium in section 2-2 (in the y-direction):

$$P_4 + P_6 = \tau_{xy} \cdot l_2 \cdot t = -\frac{1}{2} \cdot G \cdot t \tag{2.20}$$

The consistent solution is chosen, see section 2.4.

$$\begin{aligned} P_2 &= \frac{1}{4} \cdot G \cdot t \\ P_4 &= -\frac{1}{4} \cdot G \cdot t \\ P_6 &= -\frac{1}{4} \cdot G \cdot t \\ P_8 &= \frac{1}{4} \cdot G \cdot t \end{aligned} \tag{2.21}$$

Similar to the above method, the contributions from the shear stiffnesses to the elements k_{2j}, k_{3j}, ..., k_{8j} are found.

The element stiffness matrix for the HP disk element can now be determined, see equation **(2.22-23)**.

$$\underline{k} = \begin{bmatrix} k_1+k_5 & k_7 & -k_1+k_5 & -k_7 & -k_5 & -k_7 & -k_5 & k_7 \\ k_7 & k_4+k_6 & k_7 & -k_6 & -k_7 & -k_6 & -k_7 & -k_4+k_6 \\ -k_1+k_5 & k_7 & k_1+k_5 & -k_7 & -k_5 & -k_7 & -k_5 & k_7 \\ -k_7 & -k_6 & -k_7 & k_2+k_6 & k_7 & -k_2+k_6 & k_7 & -k_6 \\ -k_5 & -k_7 & -k_5 & k_7 & k_3+k_5 & k_7 & -k_3+k_5 & -k_7 \\ -k_7 & -k_6 & -k_7 & -k_2+k_6 & k_7 & k_2+k_6 & k_7 & -k_6 \\ -k_5 & -k_7 & -k_5 & k_7 & -k_3+k_5 & k_7 & k_3+k_5 & -k_7 \\ k_7 & -k_4+k_6 & k_7 & -k_6 & -k_7 & -k_6 & -k_7 & k_4+k_6 \end{bmatrix} \tag{2.22}$$

$$
\begin{aligned}
k_1 &= \frac{1}{2}\cdot E_s\cdot \rho_1\cdot \frac{l_2}{l_1} \vee k_1 = \frac{1}{2}\cdot E_c\cdot t\cdot \frac{l_2}{l_1} \\
k_2 &= \frac{1}{2}\cdot E_s\cdot \rho_2\cdot \frac{l_1}{l_2} \vee k_2 = \frac{1}{2}\cdot E_c\cdot t\cdot \frac{l_1}{l_2} \\
k_3 &= \frac{1}{2}\cdot E_s\cdot \rho_3\cdot \frac{l_2}{l_1} \vee k_3 = \frac{1}{2}\cdot E_c\cdot t\cdot \frac{l_2}{l_1} \\
k_4 &= \frac{1}{2}\cdot E_s\cdot \rho_4\cdot \frac{l_1}{l_2} \vee k_4 = \frac{1}{2}\cdot E_c\cdot t\cdot \frac{l_1}{l_2} \\
k_5 &= \frac{1}{4}\cdot G\cdot t\cdot \frac{l_1}{l_2} \\
k_6 &= \frac{1}{4}\cdot G\cdot t\cdot \frac{l_2}{l_1} \\
k_7 &= \frac{1}{4}\cdot G\cdot t
\end{aligned}
\tag{2.23}
$$

2.3 Sectional Forces

From the nodal displacements, the sectional forces defined on figure 2.5, can be found.

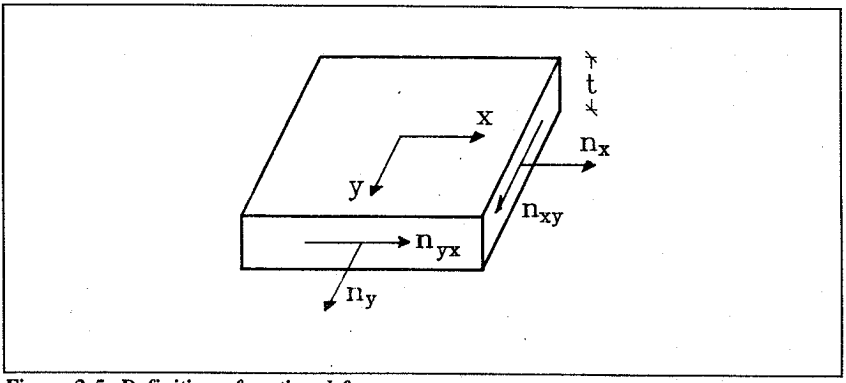

Figure 2.5: Definition of sectional forces.

The normal forces are found by multiplying the element stiffness matrixes by the element nodal displacements. This yields the normal forces in each element node.

The shear force n_{xy} is given by **(2.24)**. The change of angle ϕ_{xy} is given by **(2.6)**.

$$n_{xy} = G \cdot t \cdot \phi_{xy} = \frac{1}{2} \cdot E_c \cdot t \cdot \phi_{xy} \qquad \textbf{(2.24)}$$

2.4 Comparison with Consistent Element Formulation

In table 2.1 the corner forces P_1-P_8 ($u_5=1$, $u_i=0$, $u=[1..8] \setminus 5$) are compared with the equivalent consistent forces found by energy principles and using the displacement field **(2.25)** (coordinate system defined on figure 2.2):

$$u_x = \frac{\left(\frac{1}{2} \cdot l_1 - x\right) \cdot \left(\frac{1}{2} \cdot l_2 - y\right)}{l_1 \cdot l_2} \qquad \textbf{(2.25)}$$

$$u_y = 0$$

	HP element formulation	Consistent element formulation
P_1	$1/3 \cdot l_2/l_1 \cdot E \cdot t + 1/3 \cdot l_1/l_2 \cdot G \cdot t$	$1/2 \cdot l_2/l_1 \cdot E \cdot t + 1/4 \cdot l_1/l_2 \cdot G \cdot t$
P_2	$1/4 \cdot G \cdot t$	$1/4 \cdot G \cdot t$
P_3	$-1/3 \cdot l_2/l_1 \cdot Et \cdot 1/6 \cdot l_1/l_2 \cdot Gt$	$-1/2 \cdot l_2/l_1 \cdot E \cdot t + 1/4 \cdot l_1/l_2 \cdot G \cdot t$
P_4	$-1/4 \cdot G \cdot t$	$-1/4 \cdot G \cdot t$
P_5	$-1/6 \cdot l_2/l_1 \cdot E \cdot t - 1/6 \cdot l_1/l_2 \cdot G \cdot t$	$-1/4 \cdot l_1/L_2 \cdot G \cdot t$
P_6	$-1/4 \cdot G \cdot t$	$-1/4 \cdot G \cdot t$
P_7	$1/6 \cdot l_2/l_1 \cdot E \cdot t - 1/3 \cdot l_1/l_2 \cdot G \cdot t$	$-1/4 \cdot l_1/l_2 \cdot G \cdot t$
P_8	$1/4 \cdot G \cdot t$	$1/4 \cdot G \cdot t$

Table 2.1: Comparison of nodal forces.

If the element is given a pure axial or a pure shear deformation, the nodal forces of the HP element are equivalent to the nodal forces of the consistent element. Only in cases of combined normal and shear deformations, differences are present.

In section 4.4 a comparison between the HP element and a standard four node consistent element is presented.

Chapter 3

Implementation in FEM Programme

The HP disk element has been implemented in a FEM programme. In this chapter, the fundamentals of this programme will be described. The description is not intended as a documentation of the programme, but as a general explanation of the methods used.

For each element the reinforcement ratios in both sides and both directions, Young's Modulus for the concrete and the disk thickness can be specified. The element stiffness matrices are then found and the global stiffness matrix assembled.

As the stiffness of each element depends on whether the stringers are in tension or compression, the final solution is found by an iterative process:

1) The user can specify whether the programme assumes all stringers to be in tension or in compression in the first iteration. The element stiffness matrices are then calculated and assembled to a global stiffness matrix.
2) The global equations are solved by LU-factorization and back-substitution. Based on this solution the normal strain in each stringer is calculated.
3) For each stringer it is now examined whether the initial assumption of the stress field (tension/compression) is correct. If this assumption is not correct for all stringers, the assumptions are reversed for the stringers with a stress field being in disagreement with the first solution and a new calculation is performed based on the new stress-field.
4) The process of iteration continues until all assumptions are found to be correct. The user can specify a maximum number of iterations.

In each node, displacements and sectional forces are given as results. Furthermore, the element sectional forces and the node mean sectional forces are calculated. Finally the reactions at supported nodes are given.

Chapter 4

Numerical Examples

The element has been tested for isotropic, linear elastic material behavior in a number of problems. These will be described in the following sections. The problems examined are:

1) Fixed I-girder loaded by shear force
2) Fixed I-girder loaded by bending moment
3) Fixed solid girder loaded by shear force
4) Fixed solid girder loaded by bending moment - comparison between HP and consistent Element
5) Disk loaded by splitting force
6) Multiple span deep beam

In all of the examples the value of Young's Modulus and the disk thickness is 1.

4.1 Fixed I-girder loaded by Shear Force

As the HP disk element concentrates the normal stiffnesses in stringers along the element edges it must be expected to represent box-girders, I-girders and stiffened panels accurately, as the moment of inertia in such girders are concentrated along the edges.

Two different fixed I-girders with the following characteristics are examined.

- The depths h of both beams is 1
- The lengths l of the two beams are 8 and 4, resp.
- The finite element mesh is in both cases $(N,M)=(1,8)$
- The girders are fixed in one side
- The load P is 10

Geometry, element mesh, supports and load can be seen in figure 4.1.

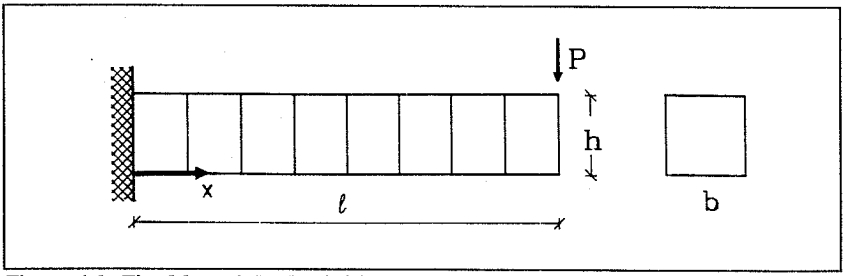

Figure 4.1: Fixed box-girder loaded by shear force.

On figure 4.2 and 4.3 the calculated deflections are compared with the exact solution for a shear beam. The maximum errors are in both cases below 0.40 percent.

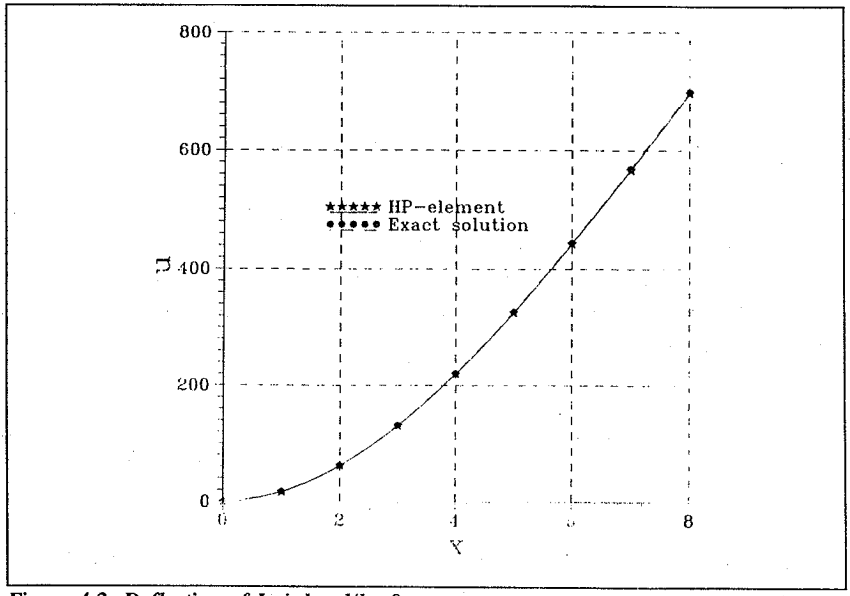

Figure 4.2: Deflection of I-girder, l/h=8.

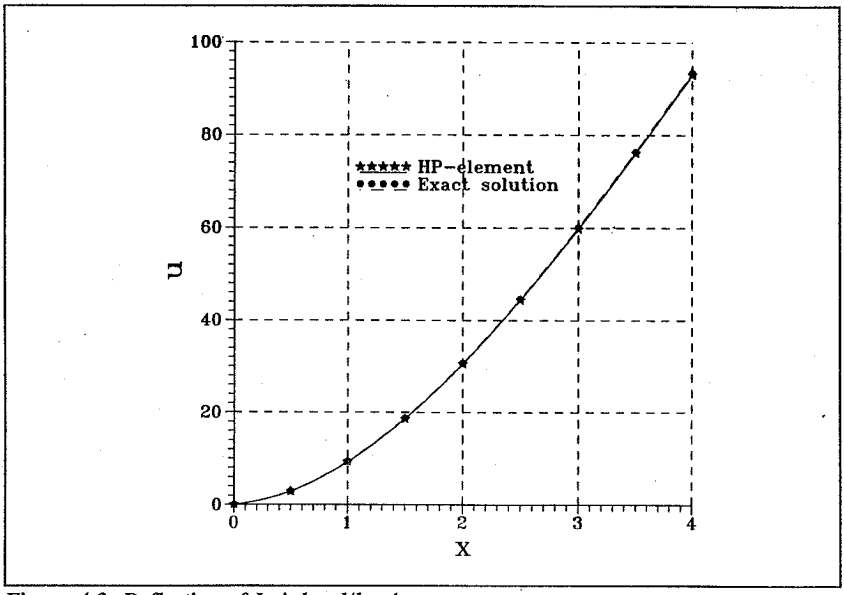

Figure 4.3: Deflection of I-girder, l/h=4.

4.2 Fixed I-girder loaded by Bending Moment

A fixed girder is loaded by a pure bending moment. This causes constant stringer forces and a constant curvature κ. When using the HP disk element for such a problem, the curvature will be exactly determined compared with Bernoulli beam theory and thus the deflection as a function of x, the distance from the support, is given by **(4.1)**:

$$u_y = \frac{1}{2} \cdot \kappa \cdot x^2 = \frac{M}{E \cdot I} \cdot x^2 \qquad \textbf{(4.1)}$$

where M is the bending moment and I the moment of inertia of the beam.

As expected, the calculated solution has been found to be in exact agreement with the theoretical solution.

4.3 Fixed solid Beam loaded by Shear Force

A solid, rectangular beam with the following characteristics is examined, see figure 4.4:

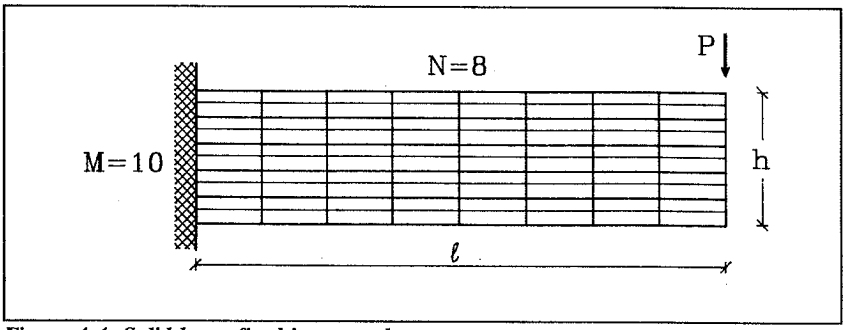

Figure 4.4: Solid beam fixed in one end.

- The depth h is 5 and the length l is 20
- An element mesh of $(N,M)=(8,10)$ is used
- The beam is fixed in one end
- The load P is 10

As the HP disk element concentrates the normal stiffnesses in stringers along the element edges the element unavoidably leads to an error in the representation of the moment of inertia of the beam. A section of a solid quadratic beam divided into N layers in the depth (same thickness) is seen on figure 4.5.

The local moment of inertia with respect to the local center of gravity for one layer is given by **(4.2)**.

$$I_{loc} = 2 \cdot b \cdot \frac{h}{2 \cdot N} \cdot \left(\frac{h}{2 \cdot N} \right)^2 \qquad \textbf{(4.2)}$$

The distance d_i to the center of gravity of layer i is given by **(4.3)**.

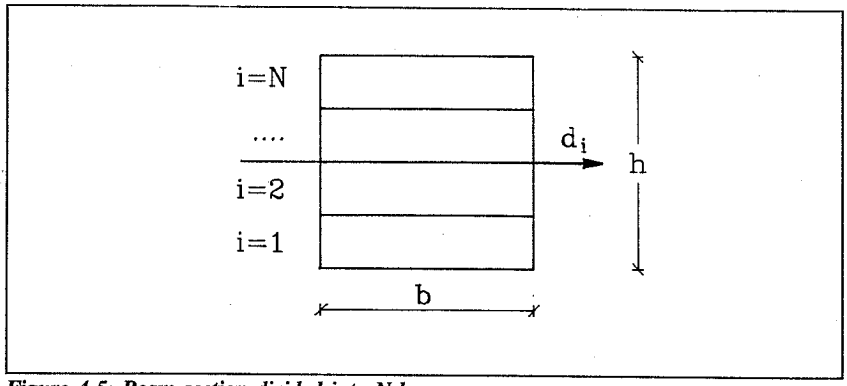

Figure 4.5: Beam section divided into N layers.

$$d_i = \left(\frac{h}{2} - \frac{h}{N}\cdot i\right) + \frac{h}{2\cdot N}\,, \quad i\in[1,2,...,N] \tag{4.3}$$

Thus the element mesh represents a moment of inertia given by **(4.4)**:

$$I = \sum_{i=1}^{N}\left[\left(\left[\frac{h}{2} - \frac{h}{N}\cdot i\right] + \frac{h}{2\cdot N}\right)^2\cdot\frac{h}{N}\cdot b + 2\cdot b\cdot\frac{h}{2\cdot N}\cdot\left(\frac{h}{2\cdot N}\right)^2\right] \tag{4.4}$$

For the examined problem, the moment of inertia calculated by **(4.4)** is $I=10.625$. The true moment of inertia is $I_t=10.4166$ so the error introduced is two percent. On figure 4.6 are shown deflections found by the FEM calculation compared with the theoretical deflections for a shear beam. The maximum error is 1.7 percent.

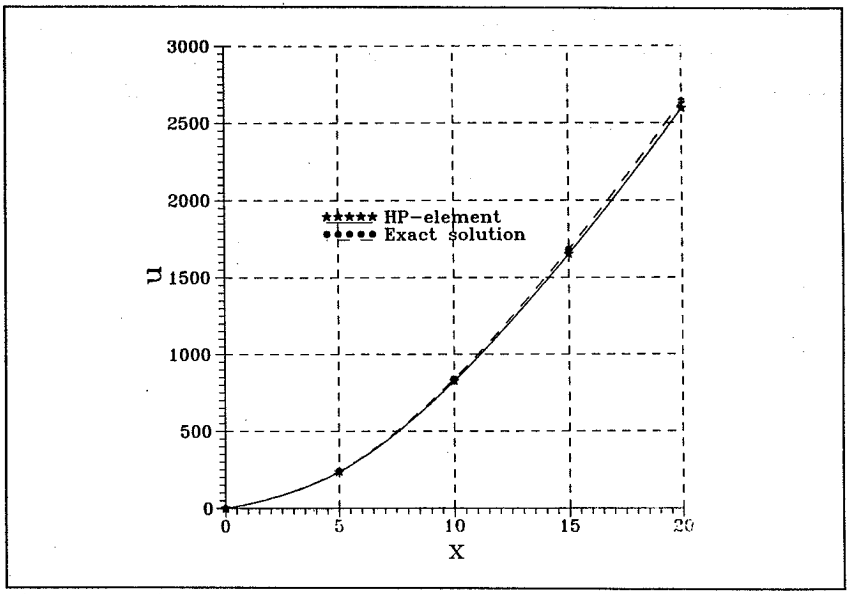

Figure 4.6: Deflection along solid beam fixed in one end.

4.4 Comparison between HP and Consistent Element

In order to examine the behavior of the HP element and a standard four node consistent element, a solid beam is examined.

- The depth h is 1 and the length l is 8
- The beam is fixed in one end
- The load is a moment load of 1 at the free end

Two analyses are performed:

- $M=10$ is kept constant, $N=\{5,10,20,49\}$
- $N=40$ is kept constant, $M=\{1,2,6,8,10\}$

N and M are defined on figure 4.4.

The deflection at the free end divided by the theoretical deflection for a Bernoulli beam n, as a function of the number of elements for the HP element and the consistent element, resp., can be seen on figure 4.7 (M constant) and figure 4.8 (N constant)

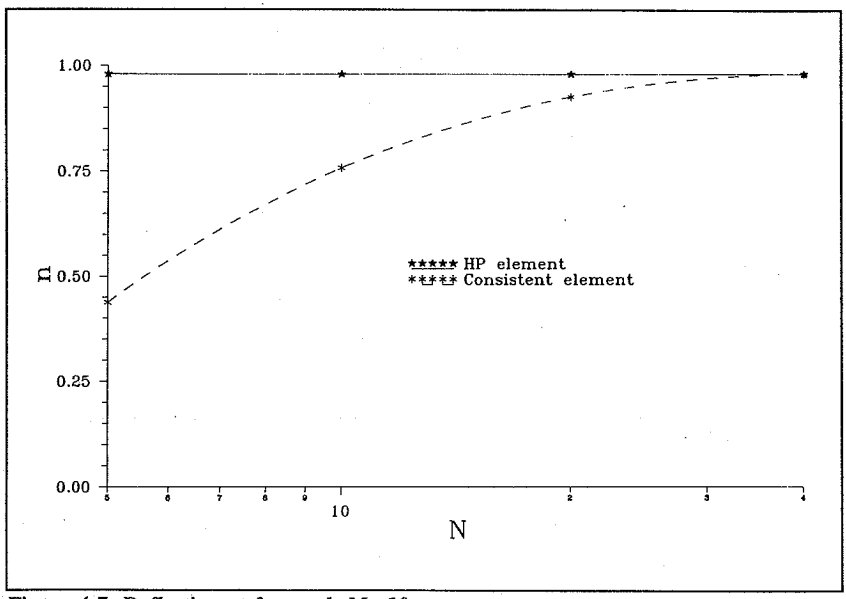

Figure 4.7: Deflection at free end, M=10.

On figure 4.7 it can be seen that for the HP element, any number of elements in the longitudinal direction yield the same result. The error is equivalent to the expected one, see section 4.3. The results from the consistent element strongly depend on the number of elements in the longitudinal direction.

For a constant number of elements in the longitudinal direction, it can be seen from figure 4.8 that the number of elements in the depth has no significance for the results yielded by the consistent element. This is due to the fact that the displacement field **(2.25)**, like in Bernoulli beam theory, assumes linear strain distribution. For decreasing values of M, the solution found by using the HP element is seen to converge against the solution that would be correct, if the beam was of box- or I-profile type, see section 4.2.

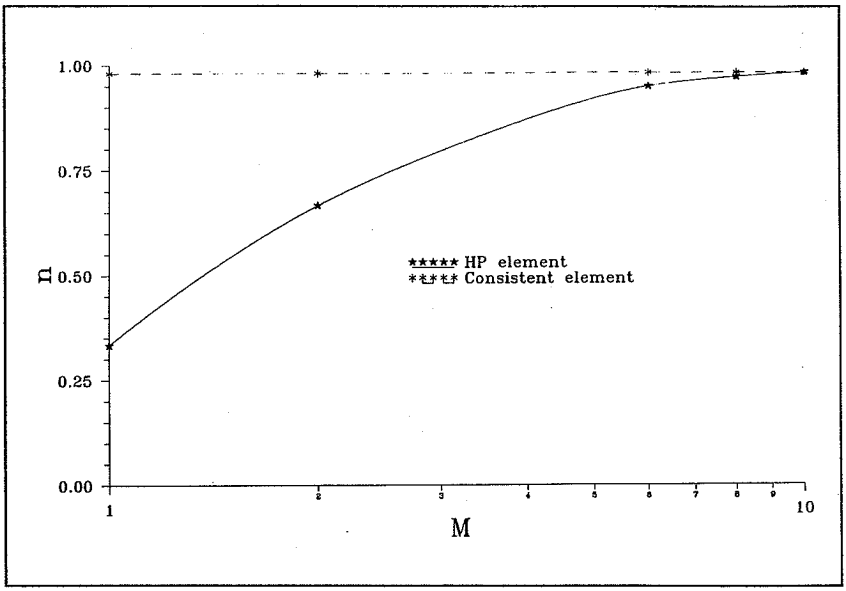

Figure 4.8: Deflection at free end, N=40.

From the results it is seen, that compared to the standard consistent element, the HP element is well suited for analyses of stringer type problems.

4.5 Disk loaded by Splitting Force

A quadratic disk is subjected to tensile stresses by applying compressive forces on two opposite edges, see figure 4.9. The problem is defined by the following parameters:

- The side length l is 5
- Due to symmetry only a quarter of the disk is modelled
- The disk is loaded by the two forces $P=2$
- An element mesh of $(N,N)=(6,6)$ is used

Splitting tests are used to determine the splitting tensile strength of concrete cylinders. A typical section of the arrangement of a splitting test of concrete cylinders can be seen in figure 4.10.

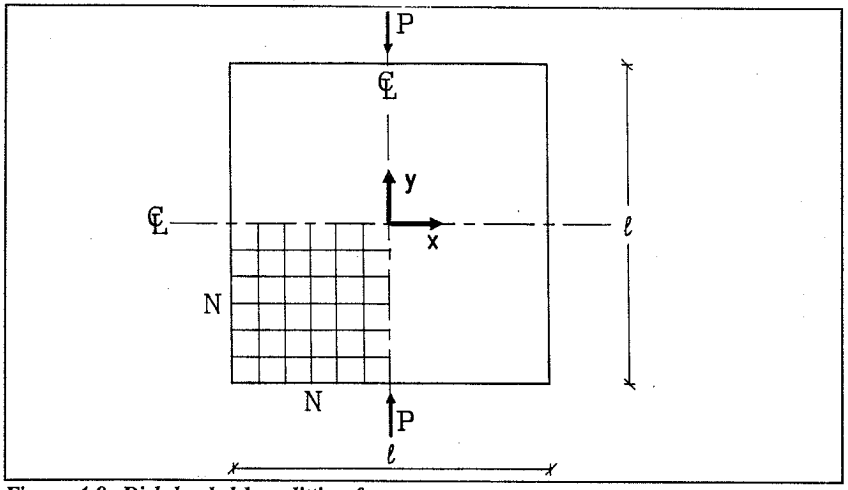

Figure 4.9: Disk loaded by splitting force.

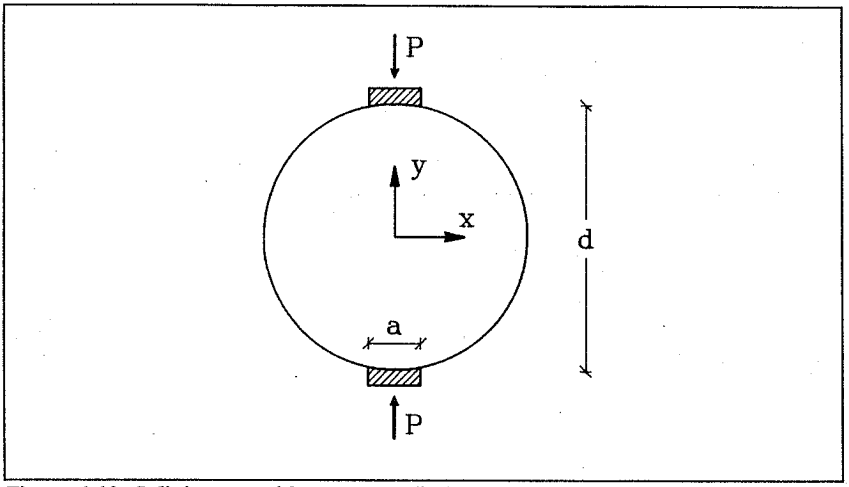

Figure 4.10: Splitting test with concrete cylinder.

The cylinder is loaded by a line load on two opposite sides. If the width a of the loading plate is less than about one tenth of the diameter d, the tensile stresses σ_x in the section through the two line loads calculated by linear elastic theory is within 1 percent given by **(4.5)**, see /6/:

$$\sigma_x = \frac{2}{\pi} \cdot \frac{P}{d} \qquad (4.5)$$

In the middle part, the results from splitting tests with cubic test specimens must be expected to be almost identical to the results from cylinders.

On figure 4.11 the results from the FEM calculation is compared with equation **(4.5)** and results found by the commercial FEM programme *ANSYS*. The results are almost identical ($l=d$).

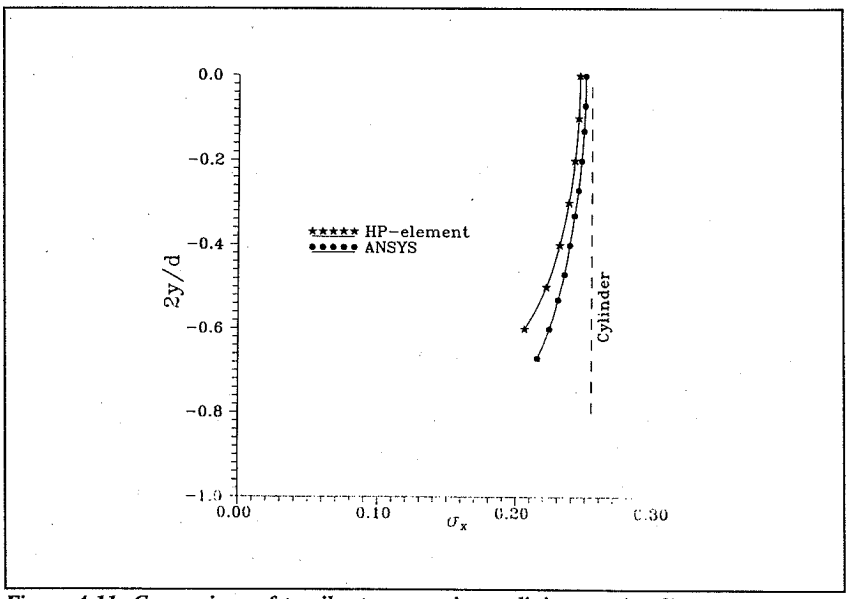

Figure 4.11: Comparison of tensile stresses σ_x in a splitting test ($x=0$).

4.6 Multiple Span Deep Beam

A multiple span deep beam loaded by an uniformly distributed load is examined, see 4.12.

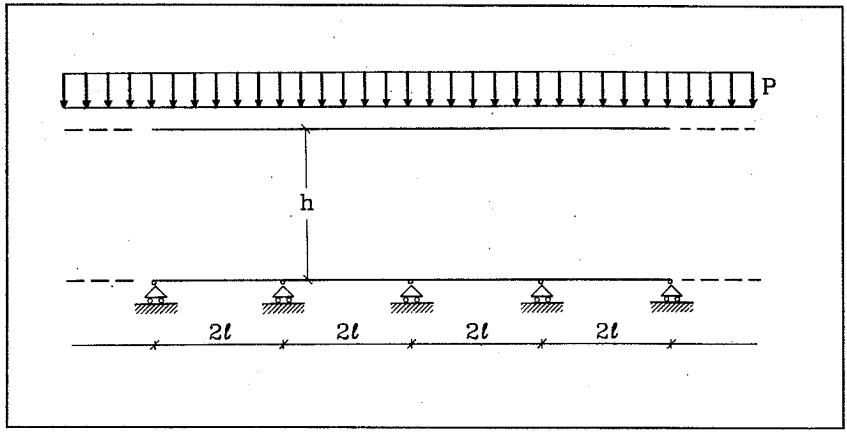

Figure 4.12: Multiple span deep beam.

If the ratio between beam depth and span is less than 2/5, results using the Navier's formula yields quite accurate results, see ref. /3/. For larger ratios, the effects of the shear strains will result in substantional errors, and such a structure should be analyzed as a plane stress problem.

Generally, a plane stress problem for an isotropic disk can be reduced to one 4th order partial differential equation **(4.6)** by introduction of Airy's stress function F. The stresses are obtained by deriving F with respect to x and y, see **(4.7)**.

$$\frac{\partial^4 F}{\partial x^4} + 2\frac{\partial^4 F}{\partial x^2 \partial y^2} + \frac{\partial^4 F}{\partial y^4} = 0 \qquad \textbf{(4.6)}$$

The solution of the compatibility equation **(4.6)** must fulfill certain boundary conditions. The problem can be solved using Fourier transformations. This was first done by *Bay*, ref. /1/ and *Dischinger*, ref. /2/. In /3/ *Theimer* used the solution method proposed by *Dischinger* to obtain solutions for a number of problems of the type shown in figure 4.12.

$$\sigma_x = \frac{\partial^2 F}{\partial y^2}$$
$$\sigma_y = \frac{\partial^2 F}{\partial x^2} \qquad (4.7)$$
$$\tau_{xy} = \tau_{yx} = -\frac{\partial^2 F}{\partial x \partial y}$$

The problem shown in figure 4.13 has been analyzed using the HP disk element.

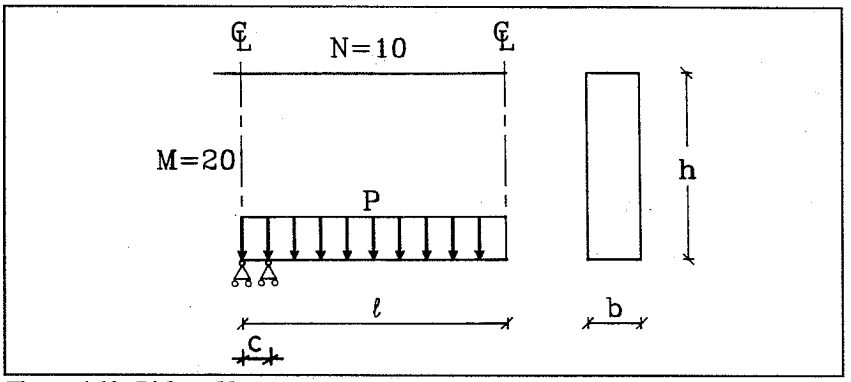

Figure 4.13: Disk problem.

The following data was used:

- *h/l*-ratios of 1 and 2/3, resp., are examined
- A line load of $p=1$ is applied along the bottom face edge
- The *b/l*-ratio is 1/10, the *c/l*-ratio is 1/10
- Due to symmetry only one half of one span is modelled
- The total number of elements is 200 *(N,M)=(10,20)*

On figures 4.14 and 4.15 the normal stresses σ_x in the vertical section in the mid of the span found by the HP disk element are compared with the theoretical solutions by *Theimer*. As seen there is a good agreement between the results.

On figures 4.16 and 4.17 σ_x in the vertical section through the middle of the support is shown. Again there is a good agreement between the results.

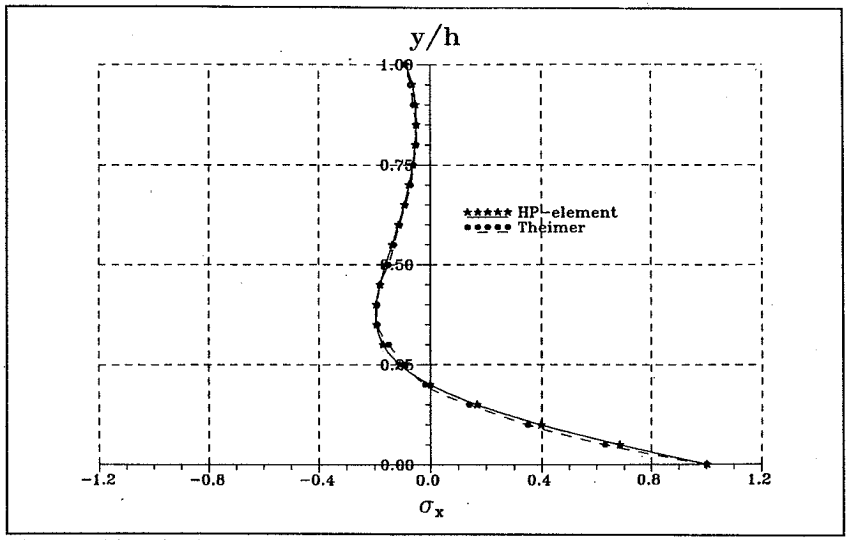

Figure 4.14: σ_x in the mid span section, h/l=1.

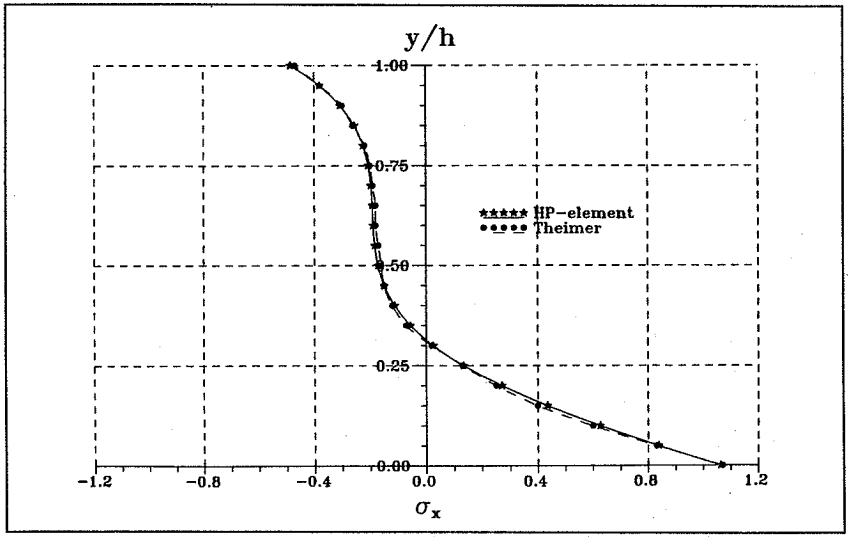

Figure 4.15: σ_x in the mid span section, h/l=2/3.

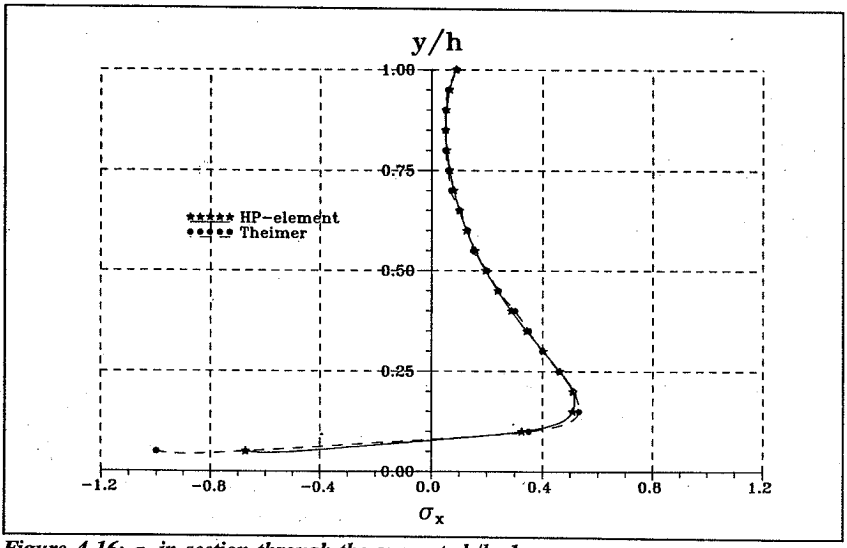

Figure 4.16: σ_x in section through the support, h/l=1.

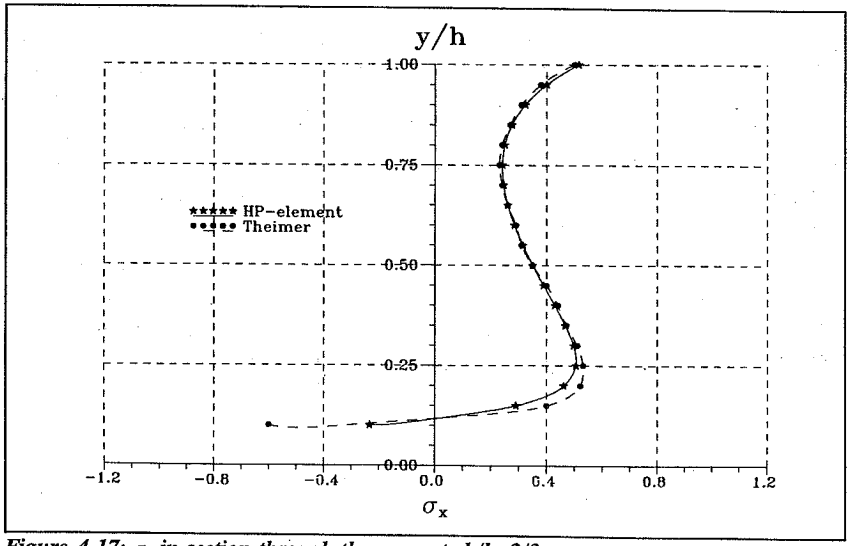

Figure 4.17: σ_x in section through the support, h/l=2/3.

Chapter 5

Conclusion

In this report a new FEM disk element called the HP disk element has been presented. The element is based on an extremely simple, mechanical model that causes normal stresses to be concentrated in stringers along the element edges and shear to be transferred by a constant in-plane shear stress field. An analytical element stiffness matrix has been derived so that numerical integration is avoided.

The element is particularly well-suited for the design of reinforced concrete disks. The behavior is very similar to the stringer method and thus input/output is of a form that can easily be converted to typical reinforcement detailing.

For each element the following input data are given: reinforcement ratios in both sides and both directions, the disk thickness and Young's Modulus for concrete. As results reactions, displacements, normal forces (unit *N/m*) and in-plane shear force (unit *N/m*) are given. The sectional forces are given for each element and as node mean forces.

The programme has been tested in a number of numerical examples and the results compared with various theoretical results as well as with another FEM programme. All the examples yield very accurate results compared with theoretical solutions taking the computational efforts into account.

Notation

a	:	Width
A_e	:	External work
A_i	:	Internal work
b	:	Width
d	:	Diameter
d_i	:	Distance to layer i
E_c	:	Young's Modulus of the concrete
E_s	:	Young's Modulus of the steel
F	:	Airy's stress function
G	:	Shear Modulus of the concrete
h	:	Depth of beam
I	:	Moment of inertia
I_t	:	Moment of inertia
$\underline{k}$	:	Element stiffness matrix
k_{ij}	:	Terms in element stiffness matrix
l	:	Length
l_1	:	Edge length of element
l_2	:	Edge lenght of element
M	:	Bending moment, integer value
N	:	Integer value
n_x	:	Normal force in x-direction
n_y	:	Normal force in y-direction
n_{xy}	:	Shear force
p	:	Line load
P	:	Concentrated load
$P_{1\text{-}8}$	:	Nodal forces
u	:	Deflection
u_x	:	Displacement in x-direction
u_y	:	Displacement in y-direction
$u_{1\text{-}8}$	:	Degrees of freedom in element
$U_{1\text{-}8}$	:	Displacements at midpoints of the four element edges

S : Normal force in stringer
t : Disk thickness
x : Coordinat direction
y : Coordinat direction

κ : Curvature
ϕ_{xy} : Shear strain
$\rho_{1\text{-}4}$: Reinforcement ratio in stringer 1-4
σ_x : Stress in x-direction
σ_y : Stress in y-direction
τ_{xy} : Shear stress

References

/1/: **H. Bay:** *"Über den Spannungszustand in hohen Trägern und die Bewehrung von Eisenbetontragwänden"* Verlag Konrad Wittwer, Stuttgart 1931

/2/: **F.Dischinger:** *"Beitrag zur Theorie der Halbscheibe und des wandartigen Trägers"* Verlag Intern, Zürich 1932

/3/: **O.F.Theimer:** *"Hilfstafeln zur Berechnung wandartiger Stahlbetonträger"* Verlag von Wilhelm Ernst & Sohn, Berlin 1967

/4/: **M.P.Nielsen:** *"Om jernbetonskivers styrke"* Polyteknisk Forlag, DTH 1969

/5/: **M.P.Nielsen:** *"Mekanik 2.1 - Plane spændings- og deformationstilstande"* Den private Ingeniørfond, DTH 1979

/6/: **H.Exner:** *"Plasticitetsteori for Coulumb Materialer"* Afdelingen for Bærende Konstruktioner R175, DTH 1983

/7/: **J.Christoffersen, L.Jagd, M.P.Nielsen:** *"HOTCH-POTCH Pladeelementet. Finite element til beregning af armerede betonplader"* Afdelingen for Bærende Konstruktioner R307, DTH 1993

AFDELINGEN FOR BÆRENDE KONSTRUKTIONER
DANMARKS TEKNISKE UNIVERSITET

Department of Structural Engineering
Technical University of Denmark, DK–2800 Lyngby

SERIE R
(Tidligere: Rapporter)

R 291. JENSEN, HENRIK ELGAARD: Creep and Shrinkage of High–Strength Concrete; A testreport; Appendix B. 1992.
R 292. JENSEN, HENRIK ELGAARD: Creep and Shrinkage of High–Strength Concrete; A testreport; Appendix C. 1992.
R 293. JENSEN, HENRIK ELGAARD: Creep and Shrinkage of High–Strength Concrete; A testreport; Appendix D. 1992.
R 294. JENSEN, HENRIK ELGAARD: Creep and Shrinkage of High–Strength Concrete; An Analysis. 1992.
R 295. JENSEN, HENRIK ELGAARD: State–of–the–art Rapport for Revnet Betons Styrke. 1992.
R 296. IBSØ, JAN BEHRENDT & RASMUSSEN, LARS JUEL: Vridning af armerede normal– og højstyrkebetonbjælker. 1992.
R 297. RIBERHOLT, HILMER, JOHANNESEN, JOHANNES MORSING & RASMUSSEN, LARS JUEL: Rammehjørner med indlimede stålstænger i limtræ. 1992.
R 298. JENSEN, RALPH BO: Modified Finite Element Method modelling Fracture Mechanical Failure in wooden beams. 1992.
R 299. IBSØ, JAN BEHRENDT & AGERSKOV, HENNING: Fatigue Life of Offshore Steel Structures under Stochastic Loading. 1992.
R 300. HANSEN, SVEND OLE: Reliability of Wind Loading on Low–Rise Buildings in a Group. 1992.
R 301. AARRE, TINE: Tensile characteristics of FRC with special emphasis on its applicability in a continuous pavement. 1992.
R 302. GLAVIND, METTE: Evaluation of the Compressive Behaviour of Fiber Reinforced High Strength Concrete. 1992.
R 303. NIELSEN, LEIF OTTO: A C ++ basis for computational mechanics software. 1993
R 304. Resuméoversigt 1992 – Summaries of Papers 1992.
R 305. HANSEN, SØREN, STANG, HENRIK: Eksperimentelt bestemte mekaniske egenskaber for fiberbeton. 1993.
R 306. NIELSEN, PER KASTRUP, ELGAARD JENSEN, HENRIK, SCHMIDT, CLAUS, NIELSEN, M.P.: Forskydning i armerede teglbjælker. 1993.
R 307. CHRISTOFFERSEN, JENS, JAGD, LARS, NIELSEN, M.P.: HOTCHPOTCH Pladeelementet – Finite element til beregning af armerede betonplader. 1993.
R 308. NIELSEN, LEIF OTTO: A C++ class library for FEM special purpose software. 1994.
R 309. DULEVSKI, ENCHO M.: Global Structural Analysis of Steel Box Girder Bridges for Various Loads. 1994.
R 310. Resuméoversigt 1993 – Summaries of Papers 1993.
R 311. JIN–PING ZHANG: Strength of Cracked Concrete. Part 1 – Shear Strength of Conventional Reinforced Concrete Beams, Deep Beams, Corbels, and Prestressed Reinforced Concrete Beams without Shear Reinforcement. 1994.
R 312. OLSEN, DAVID HOLKMANN: Fracture of Concrete A Test Series. 1994.
R 313. OLSEN, DAVID HOLKMANN: Fracture of Concrete A Test Series Appendix I. 1994.
R 314. DAHL, KAARE K.B.: Construction Joints in Normal and High Strength Concrete. 1994.
R 315. KARLSHØJ, JAN: Principper og metoder for opstilling af datamodeller til byggetekniske anvendelser. 1994.

Abonnement 1.7.1993 – 30.6.1994 kr. 130,–
Subscription rate 1.7.1993 – 30.6.1994 D.Kr. 130.–.

Hvis De ikke allerede modtager Afdelingens resuméoversigt ved udgivelsen, kan Afdelingen tilbyde at tilsende næste års resuméoversigt, når den udgives, dersom De udfylder og returnerer nedenstående kupon.

Returneres til
Afdelingen for Bærende Konstruktioner
Danmarks Tekniske Universitet
Bygning 118
2800 Lyngby

Fremtidig tilsendelse af resuméoversigter udbedes af
(bedes udfyldt med blokbogstaver):
Stilling og navn: .....
Adresse: .....
Postnr. og -distrikt: .....

The Department has pleasure in offering to send you a next year's list of summaries, free of charge. If you do not already receive it upon publication, kindly complete and return the coupon below.

To be returned to:
Department of Structural Engineering
Technical University of Denmark
Building 118
DK-2800 Lyngby, Denmark.

The undersigned wishes to receive the Department's List of Summaries:
(Please complete in block letters)
Title and name: .....
Address: .....
Postal No. and district: .....
Country: .....